TBX5 variant with the novel phenotype of mixed-type total anomalous pulmonary venous return in Holt-Oram Syndrome and variable intrafamilial heart defects

BILAL AZAB[1,2*], DUNIA ABURIZEG[2*], WEIZHEN JI[3], LAUREN JEFFRIES[3], NOOREDEEN JAMAL ISBEIH[2], AMAL SALEH AL-AKILY[2], HASHIM MOHAMMAD[2], YOUSEF ABU OSBA[2], MOHAMMAD A. SHAHIN[2], ZAIN DARDAS[4], MA'MON M. HATMAL[5], IYAD AL-AMMOURI[6] and SAQUIB LAKHANI[3]

[1]Department of Pathology and Cell Biology, Columbia University Irving Medical Center, New York, NY 10032, USA; [2]Department of Pathology and Microbiology and Forensic Medicine, School of Medicine, The University of Jordan, Amman 11942, Jordan; [3]Pediatric Genomics Discovery Program, Department of Pediatrics, Yale University School of Medicine, New Haven, CT 06504; [4]Department of Molecular and Human Genetics, Baylor College of Medicine, Houston, TX 77030, USA; [5]Department of Medical Laboratory Sciences, Faculty of Applied Medical Sciences, The Hashemite University, Zarqa 13133; [6]Department of Pediatrics, School of Medicine, The University of Jordan, Amman 11942, Jordan

Abstract. Variants in T-box transcription factor 5 (*TBX5*) can result in a wide phenotypic spectrum, specifically in the heart and the limbs. *TBX5* has been implicated in causing non-syndromic cardiac defects and Holt-Oram syndrome (HOS). The present study investigated the underlying molecular etiology of a family with heterogeneous heart defects. The proband had mixed-type total anomalous pulmonary venous return (mixed-type TAPVR), whereas her mother had an atrial septal defect. Genetic testing through trio-based whole-exome sequencing was used to reveal the molecular etiology. A nonsense variant was identified in *TBX5* (c.577G>T; p.Gly193*) initially showing co-segregation with a presumably non-syndromic presentation of congenital heart disease. Subsequent genetic investigations and more complete phenotyping led to the correct diagnosis of HOS, documenting the novel association of mixed-type TAPVR with HOS. Finally, protein modeling of the mutant TBX5 protein that harbored this pathogenic nonsense variant (p.Gly193*) revealed a substantial drop in the quantity of non-covalent bonds. The decrease in the number of non-covalent bonds suggested that the resultant mutant dimer was less stable compared with the wild-type protein, consequently affecting the protein's ability to bind DNA. The present findings extended the phenotypic cardiac defects associated with HOS; to the best of our knowledge, this is the first association of mixed-type TAPVR with *TBX5*. Prior to the current analysis, the molecular association of TAPVR with HOS had never been documented; hence, this is the first genetic investigation to report the association between TAPVR and HOS. Furthermore, it was demonstrated that the null-variants reported in the T-box domain of TBX5 were associated with a wide range of cardiac and/or skeletal anomalies on both the inter-and intrafamilial levels. In conclusion, genetic testing was highlighted as a potentially powerful approach in the prognostication of the proper diagnosis.

Correspondence to: Dr Bilal Azab, Department of Pathology and Cell Biology, Columbia University Irving Medical Center, 3959 Broadway, New York, NY 10032, USA
E-mail: ba2659@cumc.columbia.edu

Dr Saquib Lakhani, Pediatric Genomics Discovery Program, Department of Pediatrics, Yale University School of Medicine, 1 Park Street, Wing West Pavilion, New Haven, CT 06504, USA
E-mail: saquib.lakhani@yale.edu

*Contributed equally

Introduction

Congenital heart diseases (CHDs), which may have a significant impact on cardiac structure, function, or both, are the most common defects in liveborn children (1). Affecting the heart and/or great vessels, CHDs can be isolated or identified within a syndromic presentation; they are highly diverse, ranging from asymptomatic to fatal. Multiple genetic factors have been implicated in playing a role in CHDs' complex etiology (2).

Most of the known CHD causative genes encode transcription factors (TF) that assist in regulating the cardiac embryogenesis, such as NKX2-5, GATA5, TBX20, TBX1, GATA4, GATA6, TBX5, MEF2C, HAND1, NR2F2, and HAND2 (3). Among the identified TF genes are the T-box gene family, which encodes

proteins notably harboring a well-conserved T-box domain which assists in DNA binding (4). One of the T-box genes is *TBX5* (OMIM ID: 601620) that is predominantly expressed in the heart and the forelimbs (5). Pathogenic variants in *TBX5* have been associated with Holt-Oram syndrome (HOS; OMIM ID: 142900), which is characterized by congenital anomalies in both the heart and the upper limbs, in line with the TBX5 protein expression (6). Interestingly, variants in *TBX5* have also been reported to cause non-syndromic CHD (7,8). Previous observations showed that the malformations of HOS were distinctively heterogenous even among individuals sharing the same genetic variant (9-13). A wide phenotypic spectrum of septal defects, conduction abnormalities, and tetralogy of Fallot has been frequently linked to the bulk of the *TBX5*-associated heart disorders (14). However, the clinical association between HOS and total anomalous pulmonary venous return (TAPVR) has rarely been described (15).

TAPVR makes up 1-3% of the total CHD cases, with an incidence of around 7 per 100,000 live births (16). TAPVR describes the improper connection of the pulmonary veins to the right atrium or to the systemic venous system rather than the normal connection to the left atrium (17). It can also be anatomically sub-divided based on the level of the venous connection anomaly into 4 subtypes (supracardiac, infracardiac, cardiac, and mixed types) (18). To our knowledge, all the studies that claimed the association between HOS and TAPVR were only based on clinical diagnosis-no genetic testing was performed in the previous literature to confirm that *TBX5* was the implicated gene (15,19,20). Furthermore, to date, no case of mixed-type TAPVR has been reported in patients with HOS.

Over the past few years, whole-exome sequencing (WES) has been successfully implemented to uncover the underlying molecular etiology of multiple diseases. including CHD (21,22). Consequently, an accurate diagnosis of certain cases was achieved based on the identified genetic findings, which may inform families and influence patient care (23).

We present a multi-generation family affected by autosomal dominant (AD)-CHD with intrafamilial variability of specific manifestations and severity. Interestingly, the proband had a rare lethal mixed-type TAPVR. Our genetic investigation identified a hereditary disease-causing variant (DCV) in the T-box domain of *TBX5*. Consequently, the identified genetic findings prompted additional phenotyping which modified the diagnosis from non-syndromic CHD to HOS. Noteworthy, this is the first time *TBX5* has been associated with TAPVR, specifically, mixed-type TAPVR, in patients with or without HOS. Also, we aimed to augment the previously reported corpus of genetic knowledge related to null-variants in the T-box domain of *TBX5* to underpin the phenotypic intra- and interfamilial variable expressivity. Finally, we intended to illustrate the impact of harboring the variant on the protein's structure and function.

Materials and methods

Ethical compliance. This study was conducted in concordance with the tents of the Declaration of Helsinki and was approved by the Institutional Review Board (IRB) of Jordan University Hospital (protocol code 2018/198, 26 June 2018). Before enrollment, written informed consents were secured

from the participating individuals and the legal guardian (for the newborn patient).

Clinical assessment. Cardiac clinical evaluation was initially done using echocardiography (Philips HD 11 XE ultrasound system; Philips Healthcare), while the confirmation of diagnosis and detailed anatomy of the pulmonary venous drainage was achieved using contrast computed tomography (CT) scanning (Somatom Definition VA44, 2012; Siemens AG Healthcare).

Study subjects and sample collection. Blood samples were collected using EDTA tubes from the following individuals: III-1, III-2, and the proband (IV-1) (Fig. 1A). DNA isolation was conducted on the collected samples by using Wizard Genomic DNA Purification Kit (Promega) according to the manufacturer's protocol.

WES and data analysis. WES was performed on samples from parents (III-1, and III-2) and proband (IV-1). De-identified genomic DNA samples were provided to Yale under its IRB-approved protocol with a waiver of consent. Trio-exome sequencing was conducted at the Yale Center for Genomic Analysis (YCGA) through the Pediatric Genomics Discovery Program (PGDP, https://www.yalemedicine.org/departments/pediatric-genomics), a program that is freely available to coordinate sequencing, analysis, and additional testing with pediatric critical care researchers caring for children with diseases of suspected genetic etiology. Capture was performed on IDT xGen capture kit followed by Illumina DNA sequencing (HiSeq 4000) using YCGA whole-exome sequencing (WES) protocol. Paired-end sequence reads (101 bases) were converted to FASTQ format and were aligned to the reference human genome (hg19). Genetic variants were called by GATK (24), and they were annotated by ANNOVAR (25) and a custom pipeline that includes population allele frequencies, OMIM and ClinVar citations, and numerous *in silico* attributes.

The samples were sequenced to a mean depth of at least 110x independent reads per targeted base, with at least 20x independent reads in 98% of targeted bases, or 50x in 90% of targeted bases (Table SI). We filtered exonic or splice-site rare variants (MAF ≤0.01 from publicly available population databases e.g., 1000 Genomes, NHLBI-EVS, gnomAD, and our institutional database) that exhibited high quality sequence reads. *De novo* variants that were only present in the parents' samples (≥20% alternate allele ratio in the proband, alternate allele ratio <3% in parents) were called. Homozygous or compound heterozygous variants in the proband, or very rare inherited heterozygous variants from target genes were recorded (Tables SII-SV). All the recorded variants were then visualized and verified manually by Integrative Genomics Viewer (IGV). The visualization of the conserved amino acids flanking the variants was conducted by the help of UCSC browser, GRCh37/hg19 (https://genome.ucsc.edu).

Protein modeling of TBX5 (mutant and wild type). A template search with BLAST and HHBlits has been performed against the SWISS-MODEL template library (26,27). A total of 30 templates were found. Models are built based on the target-template alignment using ProMod3 (28). Coordinates that are conserved between the target and the template are
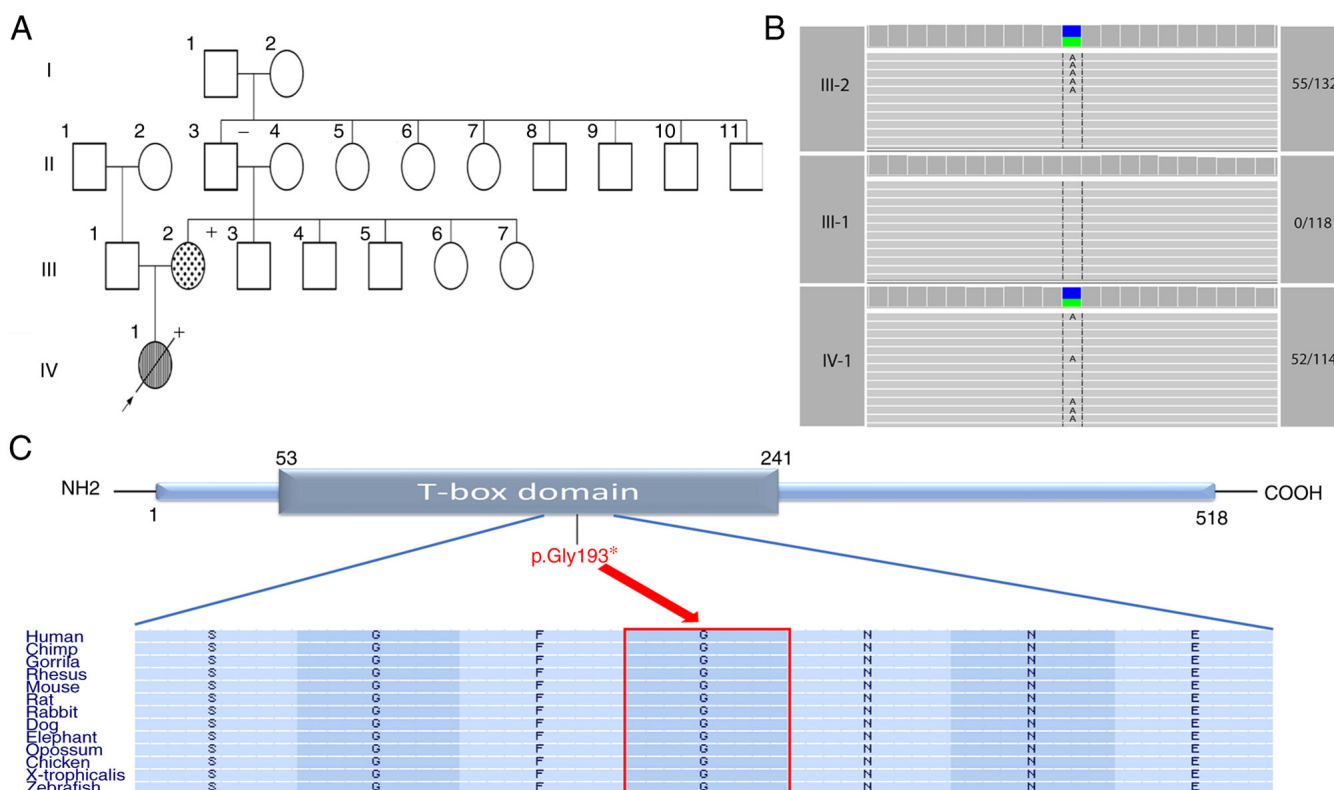
Figure 1. Description of the participating family and the identified variant. (A) Pedigree of the participating family shows the affected and unaffected family members across two generations (III-IV). The striped symbol indicates that the individual is affected by mixed-type total anomalous pulmonary venous return, while the dot-filled symbol represents the affected member with atrial septal defect. The + signs, which are located on the upper right corner of the affected individuals, indicate the presence of triphalangeal thumb. Arrow, proband; empty symbol, unaffected member; circles, females; squares, males; diagonal line, deceased member. (B) Cropped IGV screenshots showing the trio-coverage of the identified DCV in the parents and proband. The numbers on the right represent the number of reads capturing the variant over the total number of reads. (C) Schematic representation of the TBX5 protein. The identified nonsense DCV (p.Gly193*) is located within the T-box domain. The horizontal rectangle at the bottom represents the amino acid alignment around the variated residue and their corresponding conservation among selected species, created by the UCSC browser (https://genome.ucsc.edu). The arrow points towards the altered glycine residue which is highly conserved across various species. NH2 and COOH represent amino- and carboxyl-terminus, respectively.

copied from the template to the model. Insertions and deletions are remodeled using a fragment library. The sidechains are then rebuilt. Finally, the geometry of the resulting model is regularized by using a force field. In case loop modeling with ProMod3 fails, an alternative model is built with PROMOD-II (29). The global and per-residue model quality has been assessed using tools implemented in SWISSS-MODEL, including QMEAN (Qualitative Model Energy Analysis) score and MolProbity score (30). The former is a composite of 6 energy values within the homology model matrix related to protein nativeness, with score values $\leq$-4.0 indicating poor quality homology models. The latter, on the other hand, combines several protein parameters, including clash score, Ramachandran Plot criteria (Ramachandran Favored and Ramachandran Outliers) (31).
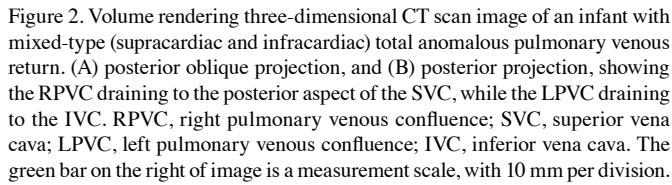
Results

Initial clinical history. The proband (IV-1; Fig. 1A) was a 12-day-old female infant who presented to the emergency room with cyanosis and respiratory distress. Physical examination showed a cyanotic infant with tachypnea and tachycardia. She had no apparent dysmorphic facial features. Evaluation by chest radiography showed a normal-sized heart with bilateral pulmonary congestion. The echocardiographic evaluation showed mixed-type TAPVR, with obstruction of pulmonary

venous drainage. There was a drainage of the pulmonary vein to the posterior aspect of the superior vena cava (SVC), with significant obstruction at its entry. In addition, pulmonary venous flow was also seen draining below the diaphragm to the inferior caval vein. The right ventricle (RV) was dilated and hypertrophic with moderate tricuspid regurgitation. The left atrium (LA) was small with right to left shunt at the atrial septum. Left ventricle appeared adequate in size with normal function. The ventricular septum was intact.

The infant was admitted to the pediatric intensive care unit on supplementary oxygen, and a CT angiogram was done the following day to confirm the complex pulmonary venous anatomy (Fig. 2). CT scan showed that the right pulmonary venous confluence (RPVC) drained to the postero-rightward aspect of the superior caval vein, and the left-sided venous confluence (LPVC) coursed behind the left atrium and descended through the diaphragm and drained to the inferior caval vein via a tortuous route (Fig. 2). The patient was transferred to the cardiac center for urgent surgical repair, but unfortunately, at the age of one month, she died before surgery from respiratory failure.

The proband (IV-1), who is the only child in this family, had a family history of CHD from the maternal lineage as it was revealed that her mother (III-2) had ostium secundum atrial septal defect (ASD) for which she underwent surgical

Figure 2. Volume rendering three-dimensional CT scan image of an infant with mixed-type (supracardiac and infracardiac) total anomalous pulmonary venous return. (A) posterior oblique projection, and (B) posterior projection, showing the RPVC draining to the posterior aspect of the SVC, while the LPVC draining to the IVC. RPVC, right pulmonary venous confluence; SVC, superior vena cava; LPVC, left pulmonary venous confluence; IVC, inferior vena cava. The green bar on the right of image is a measurement scale, with 10 mm per division.

repair during childhood (Fig. 1A). Noteworthy, no clinical examinations were done for the distant family members, and the data of their clinical status were based on the provided history.

Genetic analysis. As a rare cardiac anomaly, the finding of TAPVR triggered a genetic workup to better understand this abnormal clinical presentation on the molecular level. The affected proband (IV-1) along with her parents (III-1 and III-2) (Fig. 1A) underwent WES. The trio-based WES analysis revealed a maternally inherited heterozygous nonsense DCV in the *TBX5* gene (Table I and Fig. 1B). This DCV (c.577G>T; p.Gly193*) is located in exon 6 at an evolutionarily highly conserved position (GERP score=5.75). Also, this variant is located within the T-box domain of the TBX5 protein (Fig. 1C).

The characteristics and classification of the identified DCV. This DCV in *TBX5* (c.577G>T) introduces a stop codon at residue number 193 (p.Gly193*; Table I) of the resultant protein. This premature termination codon (PTC) can lead to the translation of an aberrant short protein-the last 325 amino acids (35% of the protein length) might be lost. Potential nonsense-mediated mRNA decay (NMD) is also a predicted mechanism as the distance between the mRNA's stop codon and the nearest 3'-end of the exon-exon junction is more than 55 nucleotides long. This DCV is absent from the population database (gnomAD; https://gnomad.broadinstitute.org). It has been previously reported in a Chinese Han family with multiple affected individuals with CHDs (32). ClinVar has no prior entry for this variant. Multiple loss-of-function (LoF) variants in *TBX5* have been already reported to be disease-causing. Given together, according to the ACMG guidelines (Richards *et al* 2015), we classify this DCV as pathogenic (Table I) (33). This is the first finding for *TBX5* to be associated with the complex cardiac manifestation of mixed-type TAPVR.

Protein modeling of the wild type and mutant (p.Gly193) versions of TBX5.* The resulting homology structure was evaluated employing structure assessment tools within SWISS-MODEL. The results are as follows (in brackets):

Table I. Details of the identified disease-causing variant.

Gene	Variant coordinate	RefSeq transcript	Exon	HGVS cDNA	HGVS aa	Consequence	Zygosity	Highest MAF in gnomAD V2, V3	ClinVar	ACMG classification (Richards *et al* 2015) (33)
TBX5	GRCh37 (hg19) chr12:114832632 GRCh38 (hg38) chr12:114394827	NM_181486.4	6/9	c.577G>T	p.Gly193*	Nonsense	HET	Not found	Not reported	Pathogenic

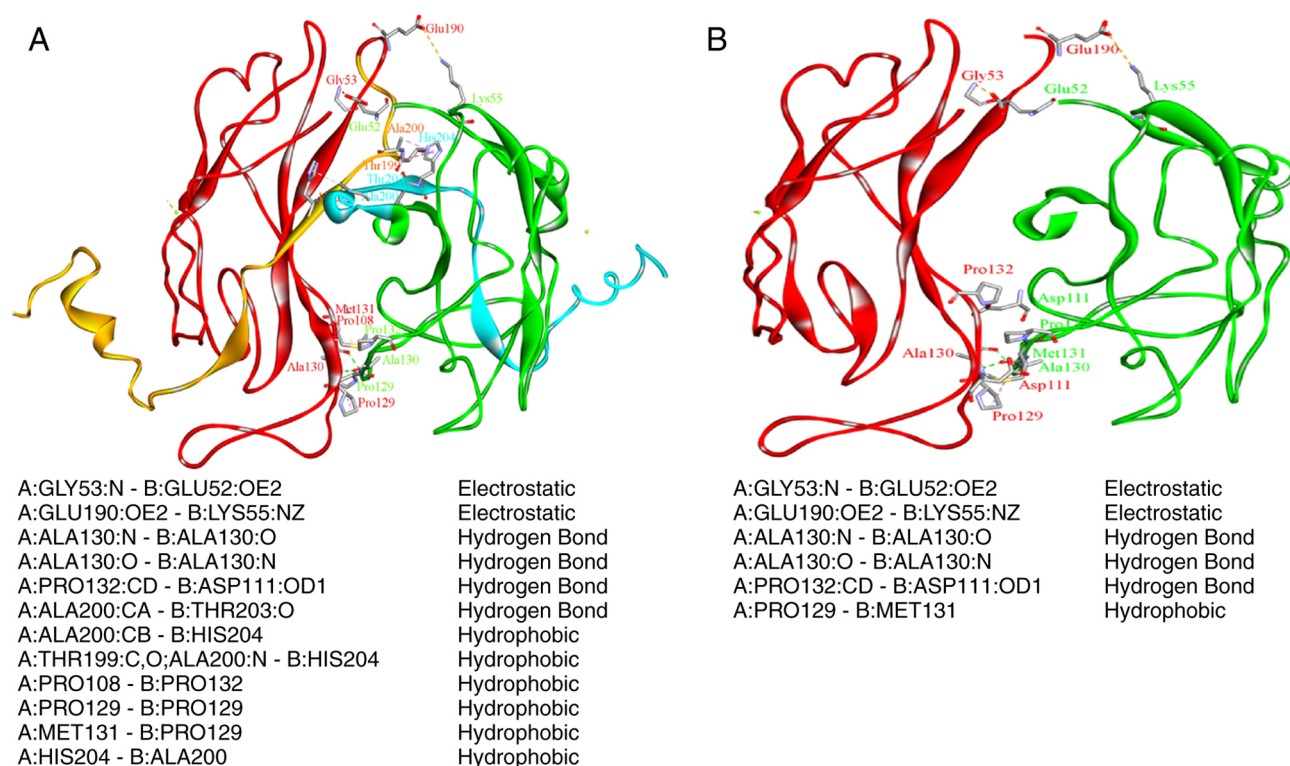MAF, minor allele frequency; V, version; HET, heterozygous.

A:GLY53:N - B:GLU52:OE2	Electrostatic
A:GLU190:OE2 - B:LYS55:NZ	Electrostatic
A:ALA130:N - B:ALA130:O	Hydrogen Bond
A:ALA130:O - B:ALA130:N	Hydrogen Bond
A:PRO132:CD - B:ASP111:OD1	Hydrogen Bond
A:ALA200:CA - B:THR203:O	Hydrogen Bond
A:ALA200:CB - B:HIS204	Hydrophobic
A:THR199:C,O;ALA200:N - B:HIS204	Hydrophobic
A:PRO108 - B:PRO132	Hydrophobic
A:PRO129 - B:PRO129	Hydrophobic
A:MET131 - B:PRO129	Hydrophobic
A:HIS204 - B:ALA200	Hydrophobic

A:GLY53:N - B:GLU52:OE2	Electrostatic
A:GLU190:OE2 - B:LYS55:NZ	Electrostatic
A:ALA130:N - B:ALA130:O	Hydrogen Bond
A:ALA130:O - B:ALA130:N	Hydrogen Bond
A:PRO132:CD - B:ASP111:OD1	Hydrogen Bond
A:PRO129 - B:MET131	Hydrophobic

Figure 3. Interactions between the two units of the TBX5 dimer in wild type and mutant forms are different. Orange and cyan represent homologous parts in the dimer that are present in the wild-type protein but are absent in the mutant protein. Red and green units show the two monomer units of the dimer. Presence of the parts marked in orange and cyan for the red and green units, respectively, distinguishes the wild form dimer from the mutant version. (A) Interaction between the two units in wild form is shown. (B) A shortened dimer in mutant form with orange and cyan portions missing. The number of non-covalent bonds (interactions) decreased dramatically.

QMEAN (-0.30), MolProbity score (1.5), Clash score (1.17), Ramachandran Favored (96.42%). The truncated protein was prepared using Discovery Studio (version 4.5). Both wild type (WT) and mutated proteins (in dimer forms) were minimized for 10 steps using Discovery Studio (version 4.5), and then the non-bond interactions between the two units were identified using the implemented tool in Discovery Studio (version 4.5). Fig. 3 shows the significant reduction in the number of non-covalent bond interactions, which clarifies the less stabile state of the mutated dimer form. A significant reduction in the number of non-covalent bonds (interactions) may affect the stability of the dimer formation and thus its binding to DNA.

Outcome of identifying the DCV. Our genetic analysis and interpretation revealed *TBX5* as the underlying genetic etiology of the proband's disease. This finding granted re-evaluating the clinical diagnosis of the proband's non-syndromic cardiac anomaly to be part of a manifestation of HOS. A thorough assessment of the family's medical history revealed that the mother (III-2; Fig. 1), carrying the same variant, does indeed have a triphalangeal thumb in her left hand (Fig. 4). In addition, the mother declared the same bilateral thumb anomaly in her deceased child (IV-1).

The finding of triphalangeal thumb in the proband (IV-1) and her affected mother (III-2), along with their respective CHDs, suggested manifestations of HOS in the setting of a DCV in *TBX5*. This is the first documented HOS patient with the cardiac anomaly of mixed-type TAPVR (Fig. 2).

Figure 4. Pictures of the mother's hand (III-2) showing the associated skeletal anomaly. (A) Unilateral triphalangeal thumb of the left hand in the mother. (B) Palmar aspect of the left-hand shows the anomaly. The thumb is long and has three phalanges.

Discussion

The *TBX5* gene encodes for a transcriptional factor protein belonging to the T-box protein family and plays a major role in regulating the early cardiac and upper limb developmental processes (34). Interestingly, TBX5 interacts with other 'cardiac-critical' transcriptional factors, such as NKX2-5 and GATA4, which both also help in the early stages of the heart development pathways (35). Thus, genetic variations in the *TBX5* can lead to both cardiac and/or skeletal defects (36). Variants in *TBX5* cause HOS, also known as the heart-hand syndrome, which is inherited as an AD trait (6).

In this study, we identified the underlying genetic etiology behind a family with AD-CHDs in which the index case presented with mixed-type TAPVR while her mother had ASD. After conducting a trio-based WES analysis, we identified a maternally inherited pathogenic DCV in *TBX5*. Notably, prior

to our investigation, the proband's mother (III-2), who suffered from ASD along with triphalangeal thumb, had never been diagnosed with HOS. The genetic finding of the DCV in *TBX5* triggered us to perform a thorough review of her medical records and consequently reached her proper diagnosis with HOS.

LoF variants in *TBX5*, such as the pathogenic nonsense variant (c.577G>T; p.Gly193*) identified here, are established to be disease-causing in HOS. The resultant protein is predicted to harbor a PTC and probably would yield an aberrantly truncated protein (only 193 out of 518 TBX5's amino acid residues might be translated, representing nearly 35% of the total protein's length). The transcribed *TBX5* mRNA harboring the PTC might instead undergo degradation through the NMD process, resulting in TBX5 haploinsufficiency (37). Previous functional *in vitro* analysis for this DCV showed that the mutated TBX5 protein failed to activate its targeted genes (*MYH6*, and *NPPA*), and no synergistic transactivation between the mutated protein and other transcription factors (NKX2-5, and GATA4) was detected. The designated pathways, which are considered essential for cardiac development, could be nullified in embryos harboring this DCV and probably lead to the consequent heart defect (32). By utilizing protein modeling tools, we studied the impact of harboring this variant (p.Gly193*) on the TBX5's structure and function. The resultant TBX5 structure formed a destabilized dimer due to a significant reduction in the number of the non-covalent bonds, and its ability to bind DNA might be subsequently deteriorated.

Our findings illustrate that at the intrafamilial level, the elucidated CHD ranged from a simple cardiac manifestation (ASD) to a complex, ultimately lethal one (mixed-type TAPVR). Furthermore, the same DCV (c.577G>T; p.Gly193*) has been previously reported in a Chinese Han family variably affected by ASD and/or ventricular septal defect (VSD), bicuspid aortic valve (BA), and atrial fibrillation (AF) (32). Hence, variable expressivity of the cardiac defects accompanied by this specific DCV can be observed at both the intrafamilial and interfamilial levels, and it is widely ranging in severity, structural deficits, and functional compromise.

The nonsense DCV (c.577G>T; p.Gly193*) is located in the TBX5's T-box domain. Although pathogenic DCVs have been identified throughout the entire gene, they appear to cluster within this domain in particular (4). The T-box domain is a highly conserved domain across various species; it is also essential for interactions with other transcription factors and DNA binding (38). Therefore, we reviewed the reported clinical effects of the T-box's null variants on the expressivity of cardiac and skeletal malformations (Table II). We noticed that the cardiac defects were mainly associated with limb defects (and thus HOS) and ranged from isolated cases of septal defects (most common) to complex cases presenting with a combination of multiple cardiac manifestations, left ventricular noncompaction cardiomyopathy, conductive heart failure, and even valve anomalies. Nevertheless, this is the first time *TBX5* has been discovered to cause mixed-type TAPVR.

The associated skeletal deformities accompanied by the CHDs in HOS were mainly described in the hand and predominantly in the preaxial radial ray (Table II). Similarly, both the deceased proband (IV-1) and her mother (III-2) presented with a triphalangeal thumb, which has been frequently reported in the literature as a manifestation of HOS (Table II). Other skeletal malformations were reported to a lesser extent in the postaxial region and the other upper extremities (forearms, arms, and shoulder complex), but were rarely ascribed to the lower extremities (feet, hip, etc.), as shown in Table II.

While HOS typically features both cardiac and limb deformities, in certain instances, the severity of the accompanying malformations tends to be more pronounced either in the heart or in the limbs of the same patient. Moreover, a wide range of accompanying anomalies (whether they were cardiac or skeletal) seem to be variably expressed even among patients harboring the same DCV (Table II). Several models propose that the disease-causing mechanism and the severity levels can be attributed to disturbances in TBX5's binding to downstream protein-partners or recognizing targeted motifs that are vital to the embryo's heart and/or skeletal development, such as NKX2-5, GATA4, GATA6, TBX20, and MEF2C (38).

Although Table II shows a spectrum of the composite cardiac defects, we did not notice any correlation between the type or the location of the null-variant within the T-box domain and the consequent phenotypic severity. Broadly speaking, early studies suggested that type (missense vs. null variants) and/or the location of the DCVs could influence the severity of HOS's cardiac and skeletal manifestations (39). Nonetheless, these observations were based on a small number of cases, and inconsistencies were observed in the later-described ones (36,40). A recent study by Vanlerberghe *et al*, conducted a phenotype-genotype correlation on the largest molecular investigation of 78 HOS cases and found out that the null-variants were associated with less-severe cardiac manifestations when compared with the missense variants (9). Additionally, no relation was established between the type of the molecular variation (null-variants vs. missense) and the severity of the skeletal anomalies (9). Ultimately, as demonstrated in the family we report, variability is such to prevent predictions of phenotypic consequences based on genotype (40).

The TAPVR subtype identified here revealed both supracardiac and infracardiac venous anomalies, resulting in a mixed-typed classification of the TAPVR phenotype. The 3D CT scan of the proband's heart (IV-) showed that both the RPVC and LPVC failed to connect to the left atrium and instead drained directly into the SVC and IVC, respectively. The mixed-type TAPVR is rare amongst TAPVR cases-accounting for around 5% of the total occurrences (41). Cardiac, supracardiac, and infracardiac subtypes of TAPVR have been previously reported with HOS (15,19,20,42). To the best of our knowledge, mixed-type TAPVR has never been reported in HOS. Hence, this is the first genetic investigation to identify an HOS case with mixed-type TAPVR.

In summary, we utilized the trio-based WES approach to identify a pathogenic nonsense DCV in a family with hereditary CHDs. Also, we showed the importance of genetic testing in reaching the proper diagnosis-our findings aided the correct diagnosis of the proband's and her mother's cases with HOS. We explored the broad phenotypic spectrum of the reported null-variants within the T-box domain of TBX5. Importantly,

Table II. A summary of the T-box's null-variants that are reported in the HGMD Pro (Version 2020.4) database and their associated cardiac manifestations.

TBX5-null variant	Age at last examination, years	Relationship with proband	Sex	Reported phenotype	Associated skeletal anomalies					Cardiac features	(Refs.)
					Hands// deformity	Forearms// deformity	Arm and shoulder complex// deformity	Lower extremity// deformity	Other		
Lys88*	23 years	Proband	F	HOS	-R-TB//HP in 1st MCB and phalanges -L-TB//HP -2ndand 5th HF//middle phalanges HP	-Forearm// Pro. and sup.	None	None	None	ASD-II, and MVP with slight regurgitation	(10)
	13 years	Sister	F	HOS	-TB//Bi- proximally set -5th HF//HP and clinodactyly -2nd and 5th HF//Bi-HP of middle phalanges (R>L) -CB//Scaphoid and trapezium fusions	-Forearm// Bi-abnormal pro. and sup. (L>R)	None	None	None	MR	(10)
	42 years	Mother	F	HOS	-TB//Bi-Abs. -MCB//Bi-Abs.	-Forearm// Abnormal pro. and sup.	R-shoulder// Limited rotation	Various anomalies in 2nd, 3rd, and 4th toes	None	Atrial septal hypermobility, but no shunt	(10)
Tyr136*	46 years	Proband of Family A	F	HOS	-TB//Bi-HP (L>R)	None	-Deltoid// Bi-HP	None	None	ASD	(43)
	44 years	Family A Brother	M	HOS	-TBs//Bi-HP	None	-Deltoid// Bi-HP	None	None	ASD	(43)
	18 years	Family A Niece	F	HOS	-TB//Bi-HP	None	-Deltoid// Bi-HP	None	None	ASD	(43)
	40 years	Proband of family B	M	HOS	-L-TB//Abs.	-L-Radius// Abs. -R-Radius//HP	-Deltoid//HP	None	None	ASD	(43)
	55 years	Family B Brother	M	HOS	-TBs//Bi-abs.	None	-Deltoid//HP	None	None	ASD	(43)

Table II. Continued.

TBX5-null variant	Age at last examination, years	Relationship with proband	Sex	Reported phenotype	Associated skeletal anomalies					Cardiac features	(Refs.)
					Hands// deformity	Forearms// deformity	Arm and shoulder complex// deformity	Lower extremity// deformity	Other		
	53 years	Family B Brother	M	HOS	-L-TB//Abs. -R-TB//TF	None	-Deltoid/HP	None	None	ASD	(43)
Gln151*	ND	Proband	M	HOS	-L-TB/TF with distal phalanx ulnar deviation	None	None	None	None	ASD-II, MVI, AVB	(44)
c.243-2A>G	31 years	Proband	F	HOS	-TBs//Bi-anomaly	None	None	None	None	CHF	(45)
c.243-1G>C	2 years	Proband	F	HOS	-L 2nd and 3rd HF//Syndactyly -TBs//Bilateral agenesis -MCB/Bi-abs -1st HF//Abs phalanges	-L-arm// Phocomelia (L<R) -R-arm// Phocomelia -Radioulnar joint// Bi-HP -L-ulna//Abs. -Superior limbs// Spasticity (L>R) -Upper limbs// Hypotonia	None	-Hip//HP -Femoral-tibial angle//genu varum	-Nasal bones// HP -Trunk/ Hypotonia	ASD-II, muscular VSD, and pulmonary hypertension	(46)
c.242+1G>A	ND	ND	ND	HOS	Preaxial radial ray	None	None	None	None	VSD	(36)
c.363-1G>A	23 years	Proband	F	HOS	Present (ND)	Present (ND)	None	None	None	ASD	(42)
	ND	Mother	F	ND	ND	ND	ND	ND	ND	ASD and DCM but was not genetically tested	(42)
c.362+1G>T	ND	ND	ND	HOS	-TBs//Abs. -Wrist// Malformation -CB// disarticulation	-Radius bone// disarticulation	None	None	None	Conduction abnormality	(36)

Table II. Continued.

TBX5-null variant	Age at last examination, years	Relationship with proband	Sex	Reported phenotype	Associated skeletal anomalies					Cardiac features	(Refs.)
					Hands// deformity	Forearms// deformity	Arm and shoulder complex// deformity	Lower extremity// deformity	Other		
c.510+1G>T along with another path missense variant	ND	ND	ND	HOS	ND	ND	ND	ND	ND	ASD, VSD, CoA	(36)
c.510+5G>T	50 years	Proband (Mother)	F	HOS	-TB anomaly	None	None	None	None	ASD, LVNC	(47)
	ND	Daughter	F	HOS	-TBs//TF -CB//HP and extra CB	Radius//HP	None	None	None	ASD	(47)
c.664-1G>A	36 years	Proband	M	HOS	TBs/Bi-HP	L-radius// Deviated with HP	-Clavicles// HP -Shoulders// Narrow	None	Hemithorax//HP	ASD-II and anomalous right coronary artery	(48)
c.663+1G>C	ND	Proband (Father)	M	HOS	TB//Abs.	None	None	None	None	ASD	(49)
	3 years	Son	M	HOS	TB//TF	None	None	None	None	ASD	(49)
p.(Leu65 Glnfs*10)	8 years	Proband	M	HOS	-TBs//Bi-abs. -Bi-2nd and 5th HF//HP 2nd phalanges	-L-radius and ulna//HP -L-elbow// abnormal with subluxation	-Scapula glenoid fossae// insufficient development -Shoulders// Bi-subluxation -Humeri// Proximal epiphyseal dysplasia	None	None	VSD	(50)
p.(Asn 95Ilefs*29)	14 years	Proband	F	HOS	-L–TB//Aplastic -R–TB//TF	None	None	None	None	VSD	(45)
	16 years	Proband	F	HOS	TBs//Bi-TF	L-ulna//HP	Claviculae// Bi-HP	None	None	ASD-II, several VSDs	(45)

Table II. Continued.

| | | | | | Associated skeletal anomalies | | | | | | |
TBX5-null variant	Age at last examination, years	Relationship with proband	Sex	Reported phenotype	Hands// deformity	Forearms// deformity	Arm and shoulder complex// deformity	Lower extremity// deformity	Other	Cardiac features	(Refs.)
p.(Asp 118del)	42 years	Proband	F	HOS	None	None	None	None	None	VSD	(45)
	ND	ND	ND	Atrial fibrillation	ND	ND	ND	ND	ND	AF	(51)
p.(Pro139 Glnfs*11)	ND	Proband (Mother)	F	HOS	-Lhand// connected to the shoulder joint -Rt hand// Connected to the elbow joint -TBs//Bi-abs	-L-arm//Abs. -R-forearm// Abs.	None	None	None	ASD	(52)
	ND	Son	M	HOS	TBs//Bi-abs	-Upper limbs// Maldevelopment -Radii and ulnae//Curved	None	None	None	ASD	(52)
p.(Val153 Serfs*21)	ND	ND	F	HOS	2nd HF//Bi-abs	Bi-radius//Abs.	None	None	None	ASD	(40)
p.(Phe168 Leufs*6)	ND	Proband (Son)	M	HOS	-R-TB//TFI with ulnar deviation of the distal phalanx -L-TB//HP-TF	None	Shoulder gridle// Abnormal with limited motion	None	None	ASD-II, VSD, PDA	(44)
	ND	Mother	F	HOS	-R-TB//Abs -L-TB//HP	Forearms//Bi shortening with limited pro. and sup.	Shoulder gridle// Abnormal with limited motion	None	None	MVP, TVP regurgitation	(44)
p.(Val214 Aspfs*14)	ND	Proband (Mother)	F	HOS	TBs//Bi-HP	Bi-radial deviation	None	None	None	Normal	(44)
	ND	Son	M	HOS	TBs//Bi-HP	Bi-radial deviation	None	None	None	AVSD	(44)
p.(His 220del)	11 months	Proband	F	HOS	TBs//Bi-TF	-R-radius// Aplasia -L-radius and ulna// Shortened	None	None	Ribs//11 pairs of ribs	VSDs, AVSD, HPRV, AV-valve insufficiency, PVS	(35)

Table II. Continued.

TBX5-null variant	Age at last examination, years	Relationship with proband	Sex	Reported phenotype	Associated skeletal anomalies					Cardiac features	(Refs.)
					Hands// deformity	Forearms// deformity	Arm and shoulder complex// deformity	Lower extremity// deformity	Other		
p.(Met 242Ilefs*10)	ND	ND	ND	HOS	Radial club hand	None	None	None	None	ASD-II	(53)
p.(Arg134 Profs*49)	ND	Proband	F	HOS	TBs// Bi-digitalized	None	None	None	None	ASD	(40)
	ND	Uncle	M	HOS	TBs//Bilateral abs	R-radius//HP	None	None	None	VSD	(40)
	ND	Mother	F	HOS	TBs//Bilateral digitalized	R-radius//HP	None	None	None	ASD or VSD	(40)
	ND	Maternal grandmother	F	HOS	ND	ND	ND	ND	ND	VSD	(40)
	ND	Brother	M	HOS	-L-TB//HP -R-TB//TF	None	None	None	None	Multiple VSDs	(40)
p.(Ala143 Argfs*40)	ND	Proband	M	HOS	-L-TB// Abs. digit -R-TB// HP digit	L-radius//HP	None	None	None	ASD-II, muscular VSDs	(40)
	ND	Mother	F	HOS	TB//Bi-abs. digit	-L-ulna and radius//Abs. -R-ulna and radius//HP	L-humerus// HP	None	None	VSD	(40)
	ND	Brother	M	HOS	-R hand//Extra digit (R1) -L-TB//TF	None	None	None	None	Muscular-VSD	(40)
	ND	Maternal grandfather	M	HOS	-TB//HP	Radioulnar synostosis	None	None	None	ASD or VSD	(40)
p.(Lys126_ Arg134del)	ND	Extended family	ND	HOS	ND (Can be with or without skeletal defect)	ND	ND	ND	ND	ASDs VSDs, MVP, and others	(54)

Symbol //, separates between the skeletal anomaly and the corresponding deformity's description. Abs., absent; AF, atrial fibrillation; ASD, atrial septal defect; ASD-II, secundum atrial septal defect; AVB, atrioventricular block; AVSD, atrial-ventricular septal defect; Bi, bilateral; CB, carpel bone; CHF, conductive heart failure; CoA, coarctation of aorta; F, female; HF, hand fingers; HOS, Holt-Oram syndrome; HP, hypoplasia; HPRV, hypoplastic right ventricle; L, left; LVNC, left ventricular non-compaction; M, male; MCB, metacarpal bone; MR, mitral regurgitation; MVI, mitral valve insufficiency; MVP, mitral valve prolapse; ND ,not defined; PDA, patent ductus arteriosus; Pro., pronation; PVS, pulmonary venous stenosis; R, right; Sup., supination; TF, triphalangeal; TVP, tricuspid valve prolapse; VSD, ventricular septal defect.

we reported a patient presenting with mixed-type TAPVR; to our knowledge, this is the first study documenting the connection between the mixed-type TAPVR and HOS. Additionally, this is the first molecular investigation to ever associate TAPVR with HOS.

Acknowledgements

Funding

Availability of data and materials

The proband's high-throughput data generated or analyzed during this study are available in the NCBI SRA repository (accession number: PRJNA822821; https://www.ncbi.nlm.nih.gov/biosample/27279246).

Authors' contributions

BA, IAA and SL conceptualized the study. DA interpreted the data. WJ, LJ, NJI, ASAA, HM, YAO, MAS, ZD and MMH performed the data analysis. BA and IAA acquired funding. DA, WJ, NJI, ASAA, HM, YAO, MAS, ZD and MMH designed the methodology. BA, IAA and SL were project administrators and supervised the study. BA, WJ, LJ, NJI, ASAA, HM, YAO, MAS, ZD, IAA and SL conducted the experiments and generated data. DA prepared the figures and tables. BA and DA wrote the original draft. BA, WJ, LJ, IAA and SL wrote, reviewed and edited the manuscript. BA and DA confirm the authenticity of all the raw data. All authors have read and approved the final manuscript.

Ethics approval and consent to participate

This study was conducted in concordance with the tents of the Declaration of Helsinki and was approved by the Institutional Review Board of Jordan University Hospital (approval no. 2018/198; 26 June 2018). Before enrollment, written informed consents were secured from the participating individuals and the legal guardian (for the newborn patient).

Patient consent for publication

The proband's parents provided their consent for the publication of data.

Competing interests

The authors declare that they have no competing interests.

References

1. Triedman JK and Newburger JW: Trends in congenital heart disease: The next decade. Circulation 133: 2716-2733, 2016.

2. Diab NS, Barish S, Dong W, Zhao S, Allington G, Yu X, Kahle KT, Brueckner M and Jin SC: Molecular genetics and complex inheritance of congenital heart disease. Genes (Basel) 12: 1020, 2021.

3. Pierpont ME, Brueckner M, Chung WK, Garg V, Lacro RV, McGuire AL, Mital S, Priest JR, Pu WT, Roberts A, *et al*: Genetic basis for congenital heart disease: Revisited: A scientific statement from the american heart association. Circulation 138: e653-e711, 2018.

4. Isphording D, Leylek AM, Yeung J, Mischel A and Simon HG: T-box genes and congenital heart/limb malformations. Clin Genet 66: 253-264, 2004.

5. Bruneau BG, Logan M, Davis N, Levi T, Tabin CJ, Seidman JG and Seidman CE: Chamber-specific cardiac expression of Tbx5 and heart defects in Holt-Oram syndrome. Dev Biol 211: 100-108, 1999.

6. Basson CT, Bachinsky DR, Lin RC, Levi T, Elkins JA, Soults J, Grayzel D, Kroumpouzou E, Traill TA, Leblanc-Straceski J, *et al*: Mutations in human TBX5 [corrected] cause limb and cardiac malformation in Holt-Oram syndrome. Nat Genet 15: 30-35, 1997.

7. Marie Reamon-Buettner S and Borlak J: TBX5 mutations in non-Holt-Oram syndrome (HOS) malformed hearts. Hum Mutat 24: 104, 2004.

8. Yoshida A, Morisaki H, Nakaji M, Kitano M, Kim KS, Sagawa K, Ishikawa S, Satokata I, Mitani Y, Kato H, *et al*: Genetic mutation analysis in Japanese patients with non-syndromic congenital heart disease. J Hum Genet 61: 157-162, 2016.

9. Vanlerberghe C, Jourdain AS, Ghoumid J, Frenois F, Mezel A, Vaksmann G, Lenne B, Delobel B, Porchet N, Cormier-Daire V, *et al*: Holt-Oram syndrome: Clinical and molecular description of 78 patients with TBX5 variants. Eur J Hum Genet 27: 360-368, 2019.

10. Garavelli L, De Brasi D, Verri R, Guareschi E, Cariola F, Melis D, Calcagno G, Salvatore F, Unger S, Sebastio G, *et al*: Holt-Oram syndrome associated with anomalies of the feet. Am J Med Genet Part A 146A: 1185-1189, 2008.

11. Guo Q, Shen J, Liu Y, Pu T, Sun K and Chen S: Exome sequencing identifies a c.148-1G>C mutation of TBX5 in a Holt-Oram family with unusual genotype-phenotype correlations. Cell Physiol Biochem 37: 1066-1074, 2015.

12. Guo DF, Li RG, Yuan F, Shi HY, Hou XM, Qu XK, Xu YJ, Zhang M, Liu X, Jiang JQ, *et al*: TBX5 loss-of-function mutation contributes to atrial fibrillation and atypical Holt-Oram syndrome. Mol Med Rep 13: 4349-4356, 2016.

13. Zhou W, Zhao L, Jiang JQ, Jiang WF, Yang YQ and Qiu XB: A novel TBX5 loss-of-function mutation associated with sporadic dilated cardiomyopathy. Int J Mol Med 36: 282-288, 2015.

14. Goldmuntz E: The genetic contribution to congenital heart disease. Pediatr Clin North Am 51: 1721-1737, x, 2004.

15. Correa-Villaseñor A, Ferencz C, Boughman JA and Neill CA: Total anomalous pulmonary venous return: Familial and environmental factors. The Baltimore-Washington infant study group. Teratology 44: 415-428, 1991.

16. Karamlou T, Gurofsky R, Al Sukhni E, Coles JG, Williams WG, Caldarone CA, Van Arsdell GS and McCrindle BW: Factors associated with mortality and reoperation in 377 children with total anomalous pulmonary venous connection. Circulation 115: 1591-1598, 2007.

17. Shi X, Cheng L, Jiao X, Chen B, Li Z, Liang Y, Liu W, Wang J, Liu G, Xu Y, *et al*: Rare copy number variants identify novel genes in sporadic total anomalous pulmonary vein connection. Front Genet 9: 559, 2018.

18. Konduri A and Aggarwal S: Partial and total anomalous pulmonary venous connection. In: StatPearls [Internet]. Treasure Island (FL): StatPearls Publishing, 2021.

19. Marcus RH, Marcus BD and Levin SE: The upper limb-cardiovascular syndrome (Holt-Oram syndrome) in a South African family. S Afr Med J 67: 1013-1014, 1985.

20. Sahn DJ, Goldberg SJ, Allen HD and Canale JM: Cross-sectional echocardiographic imaging of supracardiac total anomalous pulmonary venous drainage to a vertical vein in a patient with Holt-Oram syndrome. Chest 79: 113-115, 1981.

21. Szot JO, Cuny H, Blue GM, Humphreys DT, Ip E, Harrison K, Sholler GF, Giannoulatou E, Leo P, Duncan EL, *et al*: A screening approach to identify clinically actionable variants causing congenital heart disease in exome data. Circ Genomic Precis Med 11: e001978, 2018.

22. Yang Y, Muzny DM, Reid JG, Bainbridge MN, Willis A, Ward PA, Braxton A, Beuten J, Xia F, Niu Z, *et al*: Clinical whole-exome sequencing for the diagnosis of mendelian disorders. N Engl J Med 369: 1502-1511, 2013.

23. Volk A, Conboy E, Wical B, Patterson M and Kirmani S: Whole-exome sequencing in the clinic: Lessons from six consecutive cases from the clinician's perspective. Mol Syndromol 6: 23-31, 2015.
24. McKenna A, Hanna M, Banks E, Sivachenko A, Cibulskis K, Kernytsky A, Garimella K, Altshuler D, Gabriel S, Daly M and DePristo MA: The genome analysis toolkit: A MapReduce framework for analyzing next-generation DNA sequencing data. Genome Res 20: 1297-1303, 2010.
25. Wang K, Li M and Hakonarson H: ANNOVAR: Functional annotation of genetic variants from high-throughput sequencing data. Nucleic Acids Res 38: e164, 2010.
26. Camacho C, Coulouris G, Avagyan V, Ma N, Papadopoulos J, Bealer K and Madden TL: BLAST+: Architecture and applications. BMC Bioinformatics 10: 421, 2009.
27. Remmert M, Biegert A, Hauser A and Söding J: HHblits: Lightning-fast iterative protein sequence searching by HMM-HMM alignment. Nat Methods 9: 173-175, 2011.
28. Waterhouse A, Bertoni M, Bienert S, Studer G, Tauriello G, Gumienny R, Heer FT, de Beer TAP, Rempfer C, Bordoli L, et al: SWISS-MODEL: Homology modelling of protein structures and complexes. Nucleic Acids Res 46: W296-W303, 2018.
29. Guex N, Peitsch MC and Schwede T: Automated comparative protein structure modeling with SWISS-MODEL and Swiss-PdbViewer: A historical perspective. Electrophoresis 30 (Suppl 1): S162-S173, 2009.
30. Williams CJ, Headd JJ, Moriarty NW, Prisant MG, Videau LL, Deis LN, Verma V, Keedy DA, Hintze BJ, Chen VB, et al: MolProbity: More and better reference data for improved all-atom structure validation. Protein Sci 27: 293-315, 2018.
31. Lovell SC, Davis IW, Arendall WB III, de Bakker PI, Word JM, Prisant MG, Richardson JS and Richardson DC: Structure validation by Calpha geometry: Phi,psi and Cbeta deviation. Proteins 50: 437-450, 2003.
32. Jiang WF, Xu YJ, Zhao CM, Wang XH, Qiu XB, Liu X, Wu SH and Yang YQ: A novel TBX5 mutation predisposes to familial cardiac septal defects and atrial fibrillation as well as bicuspid aortic valve. Genet Mol Biol 43: e20200142, 2020.
33. Richards S, Aziz N, Bale S, Bick D, Das S, Gastier-Foster J, Grody WW, Hegde M, Lyon E, Spector E, et al: Standards and guidelines for the interpretation of sequence variants: A joint consensus recommendation of the American college of medical genetics and genomics and the association for molecular pathology. Genet Med 17: 405-424, 2015.
34. Li QY, Newbury-Ecob RA, Terrett JA, Wilson DI, Curtis AR, Yi CH, Gebuhr T, Bullen PJ, Robson SC, Strachan T, et al: Holt-Oram syndrome is caused by mutations in TBX5, a member of the Brachyury (T) gene family. Nat Genet 15: 21-29, 1997.
35. Boogerd CJ, Dooijes D, Ilgun A, Mathijssen IB, Hordijk R, van de Laar IM, Rump P, Veenstra-Knol HE, Moorman AF, Barnett P and Postma AV: Functional analysis of novel TBX5 T-box mutations associated with Holt-Oram syndrome. Cardiovasc Res 88: 130-139, 2010.
36. McDermott DA, Bressan MC, He J, Lee JS, Aftimos S, Brueckner M, Gilbert F, Graham GE, Hannibal MC, Innis JW, et al: TBX5 genetic testing validates strict clinical criteria for Holt-Oram syndrome. Pediatr Res 58: 981-986, 2005.
37. Nogueira G, Fernandes R, García-Moreno JF and Romão L: Nonsense-mediated RNA decay and its bipolar function in cancer. Mol Cancer 20: 72, 2021.
38. Steimle JD and Moskowitz IP: TBX5: A key regulator of heart development. In: Current Topics in Developmental Biology. Vol. 122. Academic Press Inc.: Cambridge, MA, USA, pp195-221, 2017.
39. Basson CT, Huang T, Lin RC, Bachinsky DR, Weremowicz S, Vaglio A, Bruzzone R, Quadrelli R, Lerone M, Romeo G, et al: Different TBX5 interactions in heart and limb defined by Holt-Oram syndrome mutations. Proc Natl Acad Sci USA 96: 2919-2924, 1999.
40. Brassington AM, Sung SS, Toydemir RM, Le T, Roeder AD, Rutherford AE, Whitby FG, Jorde LB and Bamshad MJ: Expressivity of Holt-Oram syndrome is not predicted by TBX5 genotype. Am J Hum Genet 73: 74-85, 2003.
41. Tarniceriu CC, Hurjui LL, Tanase DM, Nedelcu AH, Gradinaru I, Ursaru M, Stefan Rudeanu A, Delianu C and Lozneanu L: The pulmonary venous return from normal to pathological-clinical correlations and review of literature. Medicina (Kaunas) 57: 293, 2021.
42. Patterson J, Coats C and McGowan R: Familial dilated cardiomyopathy associated with pathogenic TBX5 variants: Expanding the cardiac phenotype associated with Holt-Oram syndrome. Am J Med Genet Part A 182: 1725-1734, 2020.
43. Gruenauer-Kloevekorn C and Froster UG: Holt-Oram syndrome: A new mutation in the TBX5 gene in two unrelated families. Ann Genet 46: 19-23, 2003.
44. Borozdin W, Bravo Ferrer Acosta AM, Bamshad MJ, Botzenhart EM, Froster UG, Lemke J, Schinzel A, Spranger S, McGaughran J, Wand D, et al: Expanding the spectrum of TBX5 mutations in Holt-Oram syndrome: Detection of two intragenic deletions by quantitative real time PCR, and report of eight novel point mutations. Hum Mutat 27: 975-976, 2006.
45. Heinritz W, Moschik A, Kujat A, Spranger S, Heilbronner H, Demuth S, Bier A, Tihanyi M, Mundlos S, Gruenauer-Kloevekorn C and Froster UG: Identification of new mutations in the TBX5 gene in patients with Holt-Oram syndrome. Heart 91: 383-384, 2005.
46. Ríos-Serna LJ, Díaz-Ordoñez L, Candelo E and Pachajoa H: A novel de novo TBX5 mutation in a patient with Holt-oram syndrome. Appl Clin Genet 11: 157-162, 2018.
47. Ross SB, Bagnall RD, Yeates L, Sy RW and Semsarian C: Holt-Oram syndrome in two families diagnosed with left ventricular noncompaction and conduction disease. HeartRhythm Case Rep 4: 146-151, 2018.
48. Vianna CB, Miura N, Pereira AC and Jatene MB: Holt-Oram syndrome: Novel TBX5 mutation and associated anomalous right coronary artery. Cardiol Young 21: 351-353, 2011.
49. Qin L, Lou G, Guo L, Zhang Y, Wang H, Wang L, Hou Q, Liu H, Li X and Liao S: Targeted next-generation sequencing-based molecular diagnosis of congenital hand malformations in Chinese population. Sci Rep 8: 12721, 2018.
50. Atik T, Dervisoglu H, Onay H, Ozkinay F and Cogulu O: A new mutation in the TBX5 gene in Holt-Oram syndrome: Two cases in the same family and prenatal diagnosis. J Trop Pediatr 60: 257-259, 2014.
51. Ma JF, Yang F, Mahida SN, Zhao L, Chen X, Zhang ML, Sun Z, Yao Y, Zhang YX, Zheng GY, et al: TBX5 mutations contribute to early-onset atrial fibrillation in Chinese and Caucasians. Cardiovasc Res 109: 442-450, 2016.
52. Yang J, Hu D, Xia J, Yang Y, Ying B, Hu J and Zhou X: Three novel TBX5 mutations in Chinese patients with Holt-Oram syndrome. Am J Med Genet 92: 237-240, 2000.
53. Debeer P, Race V, Gewillig M, Devriendt K and Frijns JP: Novel TBX5 mutations in patients with Holt-Oram syndrome. Clin Orthop Relat Res 462: 20-26, 2007.
54. Fan C, Duhagon MA, Oberti C, Chen S, Hiroi Y, Komuro I, Duhagon PI, Canessa R and Wang Q: Novel TBX5 mutations and molecular mechanism for Holt-Oram syndrome. J Med Genet 40: e29, 2003.